

Experimental multiparticle entanglement dynamics induced by decoherence

J. T. Barreiro,¹ P. Schindler,¹ O. Gühne,^{2,3} T. Monz,¹

M. Chwalla,¹ C. F. Roos,^{1,2} M. Hennrich,¹ and R. Blatt^{1,2}

¹*Institut für Experimentalphysik, Universität Innsbruck, Technikerstr. 25, 6020 Innsbruck, Austria*

²*Institut für Quantenoptik und Quanteninformation,*

Österreichische Akademie der Wissenschaften, Technikerstr. 21A, 6020 Innsbruck, Austria

³*Institut für Theoretische Physik, Universität Innsbruck, Technikerstr. 25, 6020 Innsbruck, Austria*

Multiparticle entanglement leads to richer correlations than two-particle entanglement and gives rise to striking contradictions with local realism [1], inequivalent classes of entanglement [2], and applications such as one-way or topological quantum computing [3, 4]. When exposed to decohering or dissipative environments, multiparticle entanglement yields subtle dynamical features and access to new classes of states and applications. Here, using a string of trapped ions, we experimentally characterize the dynamics of entanglement of a multiparticle state under the influence of decoherence. By embedding an entangled state of four qubits in a decohering environment (via spontaneous decay), we observe a rich dynamics crossing distinctive domains: Bell-inequality violation, entanglement superactivation, bound entanglement, and full separability. We also develop new theoretical tools for characterizing entanglement in quantum states. Our techniques to control the environment can be used to enable novel quantum-computation, state-engineering, and simulation paradigms based on dissipation and decoherence [5–7].

When exposed to an environment, bipartite entanglement already shows subtle dynamical features, e.g., finite-time disentanglement [8, 9]. In a multipartite setting, decoherence and dissipation enable novel quantum applications [5–7], induce even more interesting dynamics due to the different classes of states, and can decrease the number of particles genuinely entangled—an effect recently observed [10]. However, decoherence can also influence many other state properties useful for quantum information processing, such as distillability and the entanglement between subsystems. A state is distillable if, using *local* operations and classical communication, one can extract the maximally entangled states required by several quantum communication protocols such as dense coding [11] and teleportation [12].

An environment can also drive a multiparticle entangled and distillable state into the undistillable but still entangled domain [13, 14], called bound entangled (BE) [15]. This class of states is expected to appear in many body systems [16], and despite of being undistillable, it is useful for entanglement superactivation [17], quantum secret sharing [18], or remote information concentration [19]. BE states have also given insights into classical information theory: a classical analog of bound entanglement, called bound information, exists [20]. Recently, a BE state was simulated with photons [21], as well as in a variant called pseudo-bound entanglement using nuclear magnetic resonance (NMR) [22].

Here, we report the experimentally-observed dynamics of entanglement and distillability in the neighborhood of a BE state under a partially decohering environment. Entanglement and distillability of a multiparty system are defined with respect to the state *bipartitions*, or abstract splits into two subsystems. Our work focuses on a four-party system which can be bi-partitioned in two

ways, either in pairs, or 2:2, and as a single party plus the rest, or 1:3. In this case, we call the state of the four particles 2:2 (1:3) *separable* if *every* 2:2 (1:3) bipartition can be written as a mixture of bipartite states $|\psi_k\rangle$,

$$\rho = \sum_k p_k |\psi_k\rangle\langle\psi_k|, \quad |\psi_k\rangle = |\eta_{\alpha\beta}^{(k)}\rangle|\eta_{\mu\nu}^{(k)}\rangle \quad \left(|\eta_{\alpha}^{(k)}\rangle|\eta_{\beta\mu\nu}^{(k)}\rangle\right),$$

and α , β , μ , and ν denote the particles. Otherwise, if every 2:2 (1:3) bipartition cannot be written as above, we call the state 2:2 (1:3) *entangled*. Regarding distillability, a state is 2:2 (1:3) distillable if, for *every* 2:2 (1:3) bipartition, a Bell pair can be distilled and each element of the pair belongs to one subsystem. An even stronger distillability property is entanglement superactivation, which in the case of a four-particle state, it enables five parties sharing two copies of the state to distill entanglement between the two parties holding a single particle [17].

Our study starts by preparing a 2:2- and 1:3-entangled state, violating a CHSH-type Bell inequality [18], and capable of entanglement superactivation. As we apply a tunable decohering environment, the state stops violating the Bell inequality. Then, only within a region of further decoherence the entanglement superactivation protocol is successful, while the 2:2 and 1:3 entanglement is preserved with even more decoherence. Increasing the decoherence eventually eliminates the entanglement in both bipartitions at different but finite times. This finite-time disentanglement behaviour is also sometimes called environment-induced sudden death of entanglement [8, 9]. Since the 2:2 entanglement disappears before the 1:3, we realize a domain, which can be called BE [13]. Similarly, a recent theoretical study showed that a four-qubit GHZ state (Greenberger-Horne-Zeilinger [1]) can decay into a BE state by becoming 2:2 undistillable

while slightly 1:3 entangled [13]. Further decoherence eventually makes the state fully separable, long before the single-particle coherence would asymptotically disappear.

Our experiment proceeds in three stages: state preparation, exposure to tunable decoherence, and state characterization. The goal of the first stage is to generate a state which decays into the domain of BE states when exposed to a partially decohering mechanism. We chose to prepare an initial state *close* to the Smolin state ρ_S [23], a known four-qubit BE state usually written as a mixture of the Bell states $\Phi^\pm = (|00\rangle \pm |11\rangle)/\sqrt{2}$ and $\Psi^\pm = (|01\rangle \pm |10\rangle)/\sqrt{2}$,

$$\rho_S = [|\Phi^+\Phi^+\rangle\langle\cdot| + |\Phi^-\Phi^-\rangle\langle\cdot| + |\Psi^+\Psi^+\rangle\langle\cdot| + |\Psi^-\Psi^-\rangle\langle\cdot|]/4, \quad (1)$$

where $|0\rangle$ and $|1\rangle$ are the qubit basis states, and we use the notation $|\chi\rangle\langle\cdot| \equiv |\chi\rangle\langle\chi|$. The Smolin state can be prepared by first noticing that it is a mixture of four GHZ-like states

$$\rho_S = [(|1111\rangle + |0000\rangle)\langle\cdot| + (|1100\rangle + |0011\rangle)\langle\cdot| + (|1010\rangle + |0101\rangle)\langle\cdot| + (|1001\rangle + |0110\rangle)\langle\cdot|]/8. \quad (2)$$

This state can be reached by applying a single-step GHZ-entangling operation to the mixture

$$\rho = [|1111\rangle\langle\cdot| + |1100\rangle\langle\cdot| + |1010\rangle\langle\cdot| + |1001\rangle\langle\cdot|]/4, \quad (3)$$

where the operation takes a state of the form $|x_1x_2x_3x_4\rangle$ into $(|x_1x_2x_3x_4\rangle + |\bar{x}_1\bar{x}_2\bar{x}_3\bar{x}_4\rangle)/\sqrt{2}$ and \bar{x}_i denotes the complement of state x_i of ion i in the computational basis. The mixture described by equation (3), in turn, can be generated by completely decohering a state in which three out of four particles are entangled,

$$|\Psi\rangle = (|1111\rangle + |1100\rangle + |1010\rangle + |1001\rangle)/2, \quad (4)$$

with the same mechanism as used in the second stage of our study. Finally, another GHZ-entangling operation and an NMR-like refocussing technique applied to the state $|1111\rangle$ generates the state in equation (4).

In the second stage, the intended rich dynamics was achieved by increasingly decohering the initial state, as described below (see also Supplementary Information). We characterized the state's entanglement and distillability in the last stage. A single criterion, the Peres-Horodecki separability criterion [24] can prove undistillability while its extension into a measure, known as negativity [25], can quantify entanglement. According to this criterion, if a state is separable then its partial transposition has no negative eigenvalues (it has a positive partial transpose, PPT). On the other hand, it has been shown that PPT states are undistillable [15]. Therefore, entangled but undistillable states, or BE states, can be detected by verifying that *every* 1:3 bipartition has a negative partial transpose (entanglement) [26], while *every*

2:2 bipartition has a PPT (undistillability) [15]. To determine the state's undistillability properties, we performed a complete tomographic reconstruction. Full knowledge of the state enabled us to also check further separability and distillability properties. Especially, we designed a novel algorithm to prove separability of the states, which is a stronger statement than undistillability (see Supplementary Information).

Our work was performed on a system of four $^{40}\text{Ca}^+$ ions confined to a string by a linear Paul trap with axial (radial) vibrational frequencies of approximately 1.2 MHz (4.4 MHz). Each ion hosts a qubit on the electronic Zeeman levels $D_{5/2}(m = -1/2)$, encoding $|0\rangle$, and $S_{1/2}(m = -1/2)$, encoding $|1\rangle$, determined by a magnetic field of ≈ 4 G. The ion string was optically pumped to the starting quantum state $|1111\rangle$ after being Doppler cooled and sideband cooled to the ground state of the axial center-of-mass (COM) mode [27]. The state of the qubits can be manipulated via (i) collective unitary operations $U(\theta, \phi) = \exp(-i\frac{\theta}{2}S_\phi)$, with $S_\phi = \sum_{k=1}^4 \sigma_\phi^{(k)}$, $\sigma_\phi^{(k)} = \cos(\phi)\sigma_x^{(k)} + \sin(\phi)\sigma_y^{(k)}$, and $\sigma_n^{(k)}$ a Pauli spin operator acting on the k th ion, (ii) single-qubit light-shift operations $Z^{(k)}(\theta) = \exp(-i\frac{\theta}{2}\sigma_z^{(k)})$, and (iii) a GHZ-entangling operation known as Mølmer-Sørensen gate [28, 29], $MS(\theta, \phi) = \exp(-i\frac{\theta}{4}S_\phi^2)$. We can prepare four-qubit GHZ states with a fidelity of 96% and perform collective unitaries and light-shift operations at a fidelity of 99%. These imperfections determine the proximity of our prepared initial state to the Smolin state. The full experimental sequence is shown in Fig. 1.

The partially decohering mechanism indicated in Figure 1 was implemented in the four steps shown in Figure 2: (i) hiding the population in $|0\rangle$ by a full coherent transfer into $S_{1/2}(m = 1/2)$; (ii) transfer of the population in $|1\rangle$ into the superposition $\sqrt{1-\gamma}|1\rangle + \sqrt{\gamma}|D_{5/2}(m = -5/2)\rangle$; (iii) quenching of the population in $D_{5/2}(m = -5/2)$ into $P_{3/2}(m = -3/2)$ by exposure to 854-nm radiation, so that it spontaneously decays to $|1\rangle$; and finally (iv) restoring the hidden population into $|0\rangle$. In this way, a fraction γ of the population in $|1\rangle$ irreversibly loses phase coherence with $|0\rangle$ by tracing over the emitted photon. In this case we call this basis-dependent partial loss of coherence *decoherence in the $|0\rangle, |1\rangle$ basis*. In our experiment, we decohere the states in the $|0\rangle \pm |1\rangle$ ($|0\rangle \pm i|1\rangle$) basis by applying the collective unitary rotations $U(\pi/2, \pi/2)$ ($U(\pi/2, 0)$) prior to the above decoherence, as shown in Fig. 1. The complete decohering step in the preparation of the intermediate state in equation (3) was performed in the computational basis with $\gamma = 1$.

The dynamics of entanglement was explored by varying the amount of decoherence γ to which the initial state was exposed (see Fig. 1). After being partially decohered, the density matrices of the prepared states $\rho(\gamma)$ were to-

mographically reconstructed (see Fig. 3). Error analysis was performed via Monte Carlo (MC) simulations over the raw data outcomes of the state tomography. The amount of entanglement and signature of undistillability of the measured states as a function of decoherence γ are shown in Figure 4; the explicit values for the most representative states are quoted in Table 1. Figure 4 also indicates other properties of the states determined independently of the plotted data (full details in Supplementary Information).

The measured initial state ($\gamma = 0$) is highly entangled in the 1:3 bipartitions ($N_{1:3} \gg 0$) and slightly entangled in the 2:2 ($N_{2:2} > 0$); in addition, it violates a CHSH-type Bell inequality and is capable of entanglement superactivation. The properties of the state already change at $\gamma = 0.06$, when the state no longer violates the tested Bell inequality. The entanglement superactivation protocol is successful in the domain of states from $\gamma = 0$ up to $\gamma = 0.12$. We show strong evidence in the Supplementary Information that all measured states from $\gamma = 0$ to $\gamma = 0.18$ are biseparable. This means that, although they are entangled with respect to any fixed 1:3 and 2:2 bipartition, they can be written as a mixture of separable states, which are separable with respect to *different* bipartitions.

The passage into bound entanglement occurs at $\gamma \approx 0.21$. While the measured state at $\gamma = 0.24$ is 2:2 separable and 1:3 entangled, the bound entanglement is arguable because a fraction of the MC samples revealed 2:2 entanglement, thus indicating insufficient statistics. By $\gamma = 0.32$, the state is now *bona fide* BE, when also all MC samples are 1:3 entangled, 2:2 undistillable, and even 2:2 separable. The change into full undistillability is heralded by the state measured at $\gamma = 0.47$ because all eigenvalues of the partial transpose were positive for every bipartition, as shown in Table I and Figure 4. However, while the measured state is fully separable, known methods failed to prove the separability of the MC samples. By $\gamma = 0.60$, we achieve full separability in the measured data and all MC samples.

We also found a BE state by decohering the initial state in *only* the $|0\rangle \pm |1\rangle$ basis, represented by the state at $\gamma' = 0.43$ (see Table I). We thus controllably realized a passage into bound entanglement in a simple decohering environment, with statistically significant entanglement in the 2:2 partitions and positivity of the eigenvalues of the 1:3 partially-transposed states.

In conclusion, we experimentally explored the dynamics of multiparticle entanglement, separability, and distillability under a tunable decohering mechanism. The influence of the environment naturally created a bound entangled state. Our investigation on the dynamics of multiparticle entanglement can be extended to observe bound entanglement on other states such as decaying GHZ states [13] or thermal states of spin models [16]. In addition, recent quantum-computing, state-engineering,

and simulation paradigms driven by dissipative or decohering environments [5–7] can benefit from the environment engineering techniques here demonstrated.

We gratefully acknowledge support by the Austrian Science Fund (FWF), the European Commission (SCALA, NAMEQUAM, QICS), the Institut für Quanteninformation GmbH, and a Marie Curie International Incoming Fellowship within the 7th European Community Framework Programme. This material is based upon work supported in part by IARPA.

Correspondence and requests for materials should be addressed to J.T.B. and O.G.

-
- [1] D. M. Greenberger, M. A. Horne, and A. Shimony, *Am. J. Phys.* **58**, 1131 (1990).
 - [2] W. Dür, G. Vidal, and J. Cirac, *Phys. Rev. A* **62**, 062314 (2000).
 - [3] R. Raussendorf and H. J. Briegel, *Phys. Rev. Lett.* **86**, 5188 (2001).
 - [4] C. Nayak et al., *Rev. Mod. Phys.* **80**, 1083 (2008).
 - [5] S. Diehl et al., *Nature Phys.* **4**, 878 (2008).
 - [6] F. Verstraete, M. M. Wolf, and J. I. Cirac, *Nature Phys.* **5**, 633 (2009).
 - [7] H. Weimer et al., *Nature Phys.* **6**, 382 (2010).
 - [8] T. Yu and J. Eberly, *Science* **323**, 598 (2009).
 - [9] M. Almeida et al., *Science* **316**, 579 (2007).
 - [10] S. Papp et al., *Science* **324**, 764 (2009).
 - [11] C. H. Bennett and S. J. Wiesner, *Phys. Rev. Lett.* **69**, 2881 (1992).
 - [12] C. H. Bennett et al., *Phys. Rev. Lett.* **70**, 1895 (1993).
 - [13] L. Aolita et al., *Phys. Rev. Lett.* **100**, 080501 (2008).
 - [14] A. Borrás et al., *Phys. Rev. A* **79**, 022108 (2009).
 - [15] M. Horodecki, P. Horodecki, and R. Horodecki, *Phys. Rev. Lett.* **80**, 5239 (1998).
 - [16] G. Tóth et al., *Phys. Rev. Lett.* **99**, 250405 (2007).
 - [17] P. W. Shor, J. A. Smolin, and A. V. Thapliyal, *Phys. Rev. Lett.* **90**, 107901 (2003).
 - [18] R. Augusiak and P. Horodecki, *Phys. Rev. A* **73**, 012318 (2006).
 - [19] M. Murao and V. Vedral, *Phys. Rev. Lett.* **86**, 352 (2001).
 - [20] A. Acín, J. I. Cirac, and L. Masanes, *Phys. Rev. Lett.* **92**, 107903 (2004).
 - [21] E. Amsellem and M. Bourennane, *Nature Phys.* **5**, 748 (2009).
 - [22] H. Kampermann et al., *Phys. Rev. A* **81**, 040304(R) (2010).
 - [23] J. A. Smolin, *Phys. Rev. A* **63**, 032306 (2001).
 - [24] A. Peres, *Phys. Rev. Lett.* **77**, 1413 (1996).
 - [25] G. Vidal and R. F. Werner, *Phys. Rev. A* **65**, 032314 (2002).
 - [26] W. Dür, J. I. Cirac, and R. Tarrach, *Phys. Rev. Lett.* **83**, 3562 (1999).
 - [27] F. Schmidt-Kaler et al., *Applied Physics B: Lasers and Optics* **77**, 789 (2003).
 - [28] K. Mølmer and A. Sørensen, *Phys. Rev. Lett.* **82**, 1835 (1999).
 - [29] C. A. Sackett et al., *Nature* **404**, 256 (2000).

TABLE I: Negativity and smallest eigenvalue of the partial transpose of representative states. The parties in the bipartitions are labelled as A, B, C, and D. The state with $\gamma' = 0.43$ was prepared by decohering in a single step, see text. Uncertainties in parentheses indicate one standard deviation, calculated from propagated statistics in the raw state identification events.

		AB:CD	AC:BD	AD:BC		A:BCD	B:ACD	C:ACD	D:ABC
$\gamma = 0$	$N_{2:2} =$	0.033(5)	0.041(5)	0.044(5)	$N_{1:3} =$	0.715(8)	0.715(8)	0.715(8)	0.716(8)
$\gamma = 0.32$	$\min[\text{eig}(\rho^{T_{2:2}})] =$	0.020(2)	0.019(2)	0.022(2)	$N_{1:3} =$	0.035(7)	0.032(8)	0.038(8)	0.045(7)
$\gamma = 0.47$	$\min[\text{eig}(\rho^{T_{2:2}})] =$	0.028(3)	0.029(3)	0.031(2)	$\min[\text{eig}(\rho^{T_{1:3}})] =$	0.019(3)	0.020(3)	0.019(3)	0.018(3)
$\gamma' = 0.43$	$\min[\text{eig}(\rho^{T_{2:2}})] =$	0.013(2)	0.011(2)	0.013(2)	$N_{1:3} =$	0.038(7)	0.039(7)	0.042(7)	0.045(7)

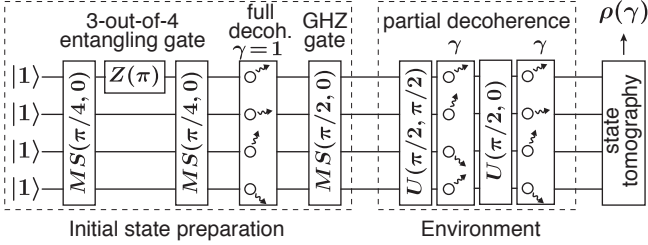


FIG. 1: Experimental sequence for studying the dynamics of multiparticle entanglement and distillability induced by decoherence. The operations indicated in the sequence are collective unitary transformations $U(\theta, \phi)$, light-shift gates $Z(\theta)$, and entangling gates $MS(\theta, \phi)$.

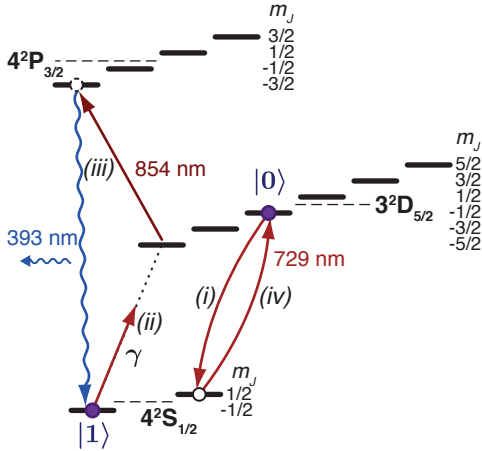


FIG. 2: Zeeman-split $^{40}\text{Ca}^+$ levels for the implementation of tunable decoherence via entanglement with a spontaneously-decaying photon. Partial decoherence is realized by simultaneously performing on all ions the steps: (i) hiding of $|0\rangle$, (ii) partial transfer of $|1\rangle$, (iii) quenching and decay of $\sqrt{\gamma}|1\rangle$, and finally (iv) restoring $|0\rangle$.

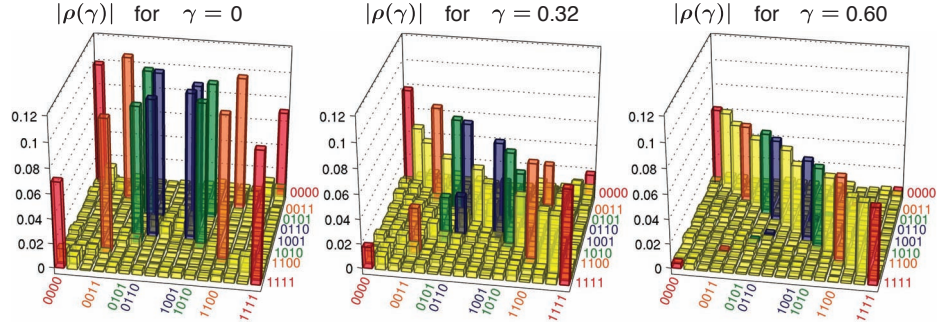


FIG. 3: Density matrices (absolute value) of states which are 2:2 and 1:3 entangled ($\gamma = 0$), bound entangled ($\gamma = 0.32$), and fully separable ($\gamma = 0.60$). The components of the Smolin state (Eq. 2) are highlighted with distinctive colors. The density matrices of all measured states are shown in the Supplementary Information.

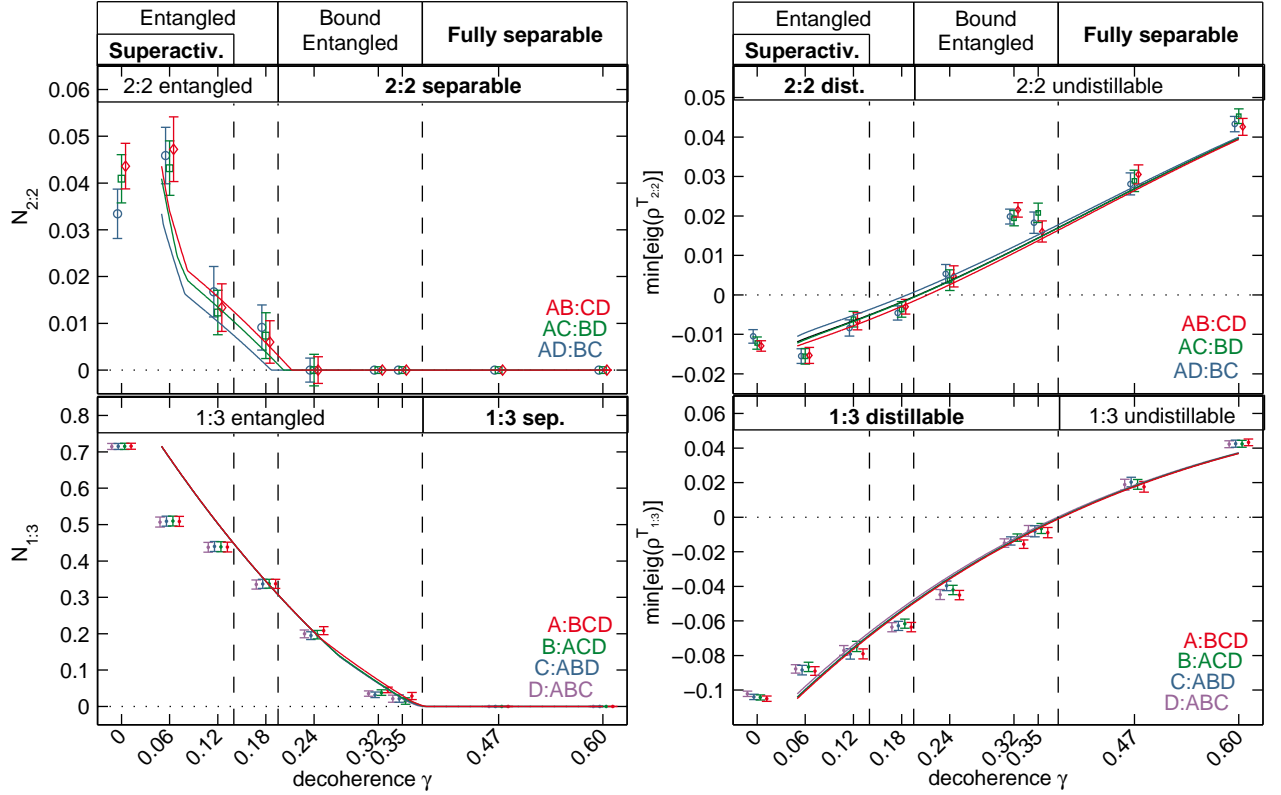


FIG. 4: Negativity and smallest eigenvalue of the partial transpose for each 2:2 and 1:3 bipartition of the measured states as a function of decoherence. A positive smallest eigenvalue of the partial transpose, $\min[\text{eig}(\rho^T)] > 0$, reveals undistillability. Bipartitions data are slightly offset horizontally for clarity, but all visible groups correspond to the same amount of decoherence indicated by the tick marks. Error bars indicate ± 1 standard deviation, calculated from propagated statistics in the raw state identification events. The solid lines were calculated by decohering the prepared initial state with a 0.05 offset in γ (due to imperfections in the decoherence implementation). The properties shown in bold were determined by tests independent of the plotted data (see Supplementary Information).

Experimental multiparticle entanglement dynamics induced by decoherence

SUPPLEMENTARY INFORMATION

J. T. Barreiro,¹ P. Schindler,¹ O. Gühne,^{2,3} T. Monz,¹
M. Chwalla,¹ C. F. Roos,^{1,2} M. Hennrich,¹ and R. Blatt^{1,2}

¹*Institut für Experimentalphysik, Universität Innsbruck, Technikerstr. 25, 6020 Innsbruck, Austria*

²*Institut für Quantenoptik und Quanteninformation,
Österreichische Akademie der Wissenschaften, Technikerstr. 21A, 6020 Innsbruck, Austria*

³*Institut für Theoretische Physik, Universität Innsbruck, Technikerstr. 25, 6020 Innsbruck, Austria*

Contents

I. Proving separability of quantum states	1
A. A direct algorithm to prove separability for a bipartite state	1
B. Proving separability for the multipartite case	2
II. Proving distillability of quantum states	3
A. Bipartite distillability	3
B. Entanglement superactivation	3
III. CHSH-type Bell inequality	3
IV. Biseparability of the states with $\gamma = 0, 0.06, 0.12$, or 0.18.	4
V. Model of imperfections reveals the observed dynamics	4
VI. Quantum state reconstruction and statistics	4
References	4

List of tables

I: Negativity and smallest eigenvalue of the partial transpose for every bipartition of the measured states	5
II: Summary of number of Monte Carlo samples satisfying the tested properties	5
III: Absolute value of measured density matrices	6
IV: Absolute value of measured density matrices after local unitaries	7

I. PROVING SEPARABILITY OF QUANTUM STATES

A. A direct algorithm to prove separability for a bipartite state

Before explaining our novel algorithm for proving separability of a quantum state, let us first define our notations and definitions. We consider a bipartite $N \times M$ system with Hilbert space $\mathcal{H} = \mathcal{H}_A \otimes \mathcal{H}_B$. Any matrix ϱ acting on \mathcal{H} which is Hermitian ($\varrho = \varrho^\dagger$), has no negative eigenvalues ($\varrho \geq 0$), and is normalized ($\text{Tr}(\varrho) = 1$) is a valid density matrix of some quantum state.

By definition, a state is separable, if it can be written as a convex combination of product states,

$$\varrho = \sum_k p_k |a_k\rangle\langle a_k| \otimes |b_k\rangle\langle b_k|, \quad (1)$$

where the p_k are non-negative ($p_k \geq 0$) and normalized ($\sum_k p_k = 1$); in other words, they form a probability distribution. If a state cannot be written as in Eq. (1) it is entangled.

For a given experimental ϱ , it is not straightforward to prove that it is separable; finding an explicit decomposition as in Eq. (1) is a hopeless task. In order to devise a simple algorithm for separability testing, we use the following two basic facts about separability:

(i) Consider a separable state ϱ_{sep} and two other states ϱ_1 and ϱ_2 such that

$$\varrho_1 = p\varrho_2 + (1-p)\varrho_{\text{sep}} \quad (2)$$

for some $p \in [0; 1]$. In this situation, if we can prove that ϱ_2 is separable, then ϱ_1 must be separable, too. This follows directly from the definition in Eq. (1), as this definition implies that the convex combination of two separable states is separable. Note that if ϱ_2 is entangled this does not mean that ϱ_1 is entangled.

(ii) If a state ϱ is close to the maximally mixed state $\varrho_m = \frac{1}{NM}\mathbb{1}$, then it is separable. Of course, a precise statement of this kind requires a specification of a distance. For this, different distances have been investigated and bounds on the distance to ϱ_m have been obtained (Braunstein *et al.*, 1999; Gurvits and Barnum, 2002, 2005; Hildebrand, 2006; Kendon *et al.*, 2002; de Vicente, 2007; Życzkowski *et al.*, 1998).

For our purposes, we will use $\text{Tr}(\varrho^2)$ as a measure of the mixedness and use the fact that if

$$\text{Tr}(\varrho^2) \leq \frac{1}{NM-1} \quad (3)$$

then ϱ is separable (Gurvits and Barnum, 2002). The maximally mixed state has $\text{Tr}(\varrho_m^2) = 1/NM$ and states with small $\text{Tr}(\varrho^2)$ are very mixed and close to the maximally mixed state.

Starting from these two facts, the basic idea of our algorithm is to find a sequence $\varrho_1, \varrho_2, \varrho_3, \dots$ such that

Eq. (2) holds for all $i, i+1$ and that $\text{Tr}(\varrho_i^2) \geq \text{Tr}(\varrho_{i+1}^2)$ holds. This sequence will lead to a minimization of $\text{Tr}(\varrho_i^2)$ and finally, Eq. (3) can be applied to prove separability of ϱ_i and hence of ϱ_1 .

In the simplest case, our algorithm can be sketched as follows:

1. Take the given experimental data ϱ_{exp} as ϱ_i with $i = 1$.
2. Consider the optimization problem

$$\max_{|\phi\rangle=|a\rangle|b\rangle} |\langle\phi|\varrho_i|\phi\rangle| \quad (4)$$

and find a product state $|\phi_i\rangle = |a_i\rangle|b_i\rangle$ which has a high overlap with ϱ_i .

Here, the aim is only to find a state with high overlap. In order to make the algorithm work one does not need a certified optimal solution of the maximization in Eq. (4) (see also below).

3. Find an ε_i with $0 \leq \varepsilon_i \leq \varepsilon_{\text{max}}$ such that

$$\varrho_{i+1} := (1 + \varepsilon_i)\varrho_i - \varepsilon_i|\phi_i\rangle\langle\phi_i| \quad (5)$$

has no negative eigenvalues and that furthermore $\text{Tr}(\varrho_i^2) \geq \text{Tr}(\varrho_{i+1}^2)$ holds. It is natural to choose ε_i such that $\text{Tr}(\varrho_{i+1}^2)$ is minimal; this is, however, not mandatory.

The point here is that if $|\phi_i\rangle$ has a high overlap with ϱ_i , then it will also have a high overlap with the eigenvector corresponding to the maximal eigenvalue $\lambda_{\text{max}}(\varrho_i)$ of ϱ_i . Then, the construction of ϱ_{i+1} is such that usually $\lambda_{\text{max}}(\varrho_{i+1}) \leq \lambda_{\text{max}}(\varrho_i)$ and, due to the normalization $\lambda_{\text{min}}(\varrho_{i+1}) \geq \lambda_{\text{min}}(\varrho_i)$ holds. Hence, ϱ_{i+1} will be closer to the maximally mixed state than ϱ_i .

4. Check, whether ϱ_{i+1} fulfills Eq. (3). If this is the case, then ϱ_{i+1} is separable and due to Eq. (2) also ϱ_i and finally ϱ_{exp} are separable. Then, the algorithm can terminate.
5. If ϱ_{i+1} does not fulfil Eq. (3) start again with step 2 and $i \mapsto i+1$ and iterate further until Eq. (3) holds for some i .

This algorithm deserves some comments:

(i) First, it is of course not guaranteed that for a separable input state the procedure will terminate at some point. Consequently, if it does not terminate after many steps, one cannot conclude that the state is entangled. It is our only claim that the algorithm outlined above is a powerful tool in practice.

In Ref. (Navascués *et al.*, 2009) an algorithm using semidefinite programming has been presented which can prove for any non-entangled state the separability after a finite number of steps. However, the number of steps

required is not known in advance, moreover, the applicability of this technique to larger Hilbert spaces or multiparticle problems is not clear. Further algorithms for separability testing have been proposed in Refs. (Hulpke and Bruß, 2005; Spedalieri, 2007); there, however, the practical implementation is still missing.

(ii) Second, note that the algorithm does not require a certified solution of any non-trivial optimization problem and that it is very robust against imperfections: Even if the computation of $|\phi_i\rangle$ or ε_i is not optimal, this does not affect the conclusion that ϱ_{exp} is separable if Eq. (3) holds at some point. Also, the ε_{max} is introduced for practical purposes, choosing a small ε_{max} makes the convergence of the algorithm better in practice.

(iii) Third, for doing the optimization in Eq. (4) note that the optimal $|\phi\rangle = |a\rangle|b\rangle$ fulfills that $|a\rangle$ is the eigenvector corresponding to the maximal eigenvalue of $X_A = \text{Tr}_B(\varrho_i \mathbb{1} \otimes |b\rangle\langle b|)$ and $|b\rangle$ is similarly vector corresponding to the maximal eigenvalue of $X_B = \text{Tr}_A(\varrho_i |a\rangle\langle a| \otimes \mathbb{1})$. This can be used to tackle the maximization iteratively: Starting from a random $|a\rangle$ one computes the optimal $|b\rangle$ via X_B , then with this $|b\rangle$ the optimal $|a'\rangle$, then again the optimal $|b'\rangle$ etc. In practice, this converges quickly towards the desired solution.

(iv) Then, one may also check during the iteration whether ϱ_i violates some of the usual entanglement criteria, e.g. the criterion of the positivity of the partial transpose. If this is the case, the iteration will never end and one can directly stop it. In this case, however, it is wrong to conclude that ϱ_{exp} was entangled.

(v) Moreover, if one wishes to find an explicit separable decomposition of ϱ as in Eq. (1) the algorithm can also help: For some of the states close to the maximally states explicit decompositions into product vectors are known (Braunstein *et al.*, 1999). Then, one can write down a decomposition consisting of this decomposition and the $|\phi_i\rangle$ in the iteration.

The algorithm outlined above can be directly implemented with few lines of code and performs very well for the states generated in the experiment.

B. Proving separability for the multipartite case

Let us now demonstrate that the ideas from above can also be used to analyze multipartite entanglement. Before doing so, we explain some basic notions about the entanglement properties of three qubits.

A pure three-qubit state $|\psi\rangle$ is fully separable, if it is of the form $|\psi\rangle = |\alpha\rangle|\beta\rangle|\gamma\rangle$ and it is biseparable, if there is a grouping of the three parties A, B , and C in two partitions (e.g. $AB|C$), such that it is separable with respect to this partition (e.g. $|\psi\rangle = |\chi\rangle_{AB}|\eta\rangle_C$). Otherwise, it is genuine tripartite entangled. For the special case of three qubits there are further two different classes of genuine tripartite entanglement: the GHZ class (represented by the GHZ state $|GHZ_3\rangle = (|000\rangle + |111\rangle)/\sqrt{2}$) and the W class (represented by the W state $|W_3\rangle =$

$(|001\rangle + |010\rangle + |100\rangle)/\sqrt{3}$). These states represent different classes of entanglement in the sense that a single copy of a W-type state cannot be converted locally in a GHZ-type state (and vice versa), even if the conversion is allowed to work only with a small probability (Dür *et al.*, 2000).

As in the bipartite case, one can extend this classification to mixed states via convex combinations: A mixed state is fully separable, if it can be written as a mixture of fully separable pure states. It is biseparable, if it can be written as a mixture of biseparable (and fully separable) states. Otherwise, it is genuine multipartite entangled. Here, it is important to note that the mixture of biseparable states may contain pure biseparable states which are biseparable with respect to different partitions. Furthermore, one can define classes of mixed W states and GHZ states (Acín *et al.*, 2001).

For a generalization of the separability algorithm it is important that similar results as Eq. (3) exist also for multipartite systems (Braunstein *et al.*, 1999; Gurvits and Barnum, 2005; Hildebrand, 2006; Kendon *et al.*, 2002). For instance, it has been shown in Ref. (Hildebrand, 2006) that if a three-qubit state fulfills

$$\text{Tr}(\varrho^2) \leq \frac{19}{136} \approx 0.1397, \quad (6)$$

then ϱ is fully separable. More generally, an N-qubit state with $N \geq 3$ is fully separable, if

$$\text{Tr}(\varrho^2) \leq \frac{1}{2^N - \alpha^2} \text{ with } \alpha^2 = \frac{2^N}{\frac{17}{2}3^{N-3} + 1} \quad (7)$$

hold. This follows also from the results of Ref. (Hildebrand, 2006), where a bound on the radius of the separable ball of unnormalized density matrices has been given, a rescaling of it delivers Eq. (7).

Given these facts one can now directly write down algorithms to prove full separability or biseparability. Finding the fully separable (or biseparable) state with the highest overlap (see Eq. (4)) can be done as before, by starting from a random fully separable (or biseparable) state and then updating it iteratively (see point (iii) above). Similarly, one can also write an algorithm which can prove that a three-qubit state belongs to the W class, since the pure W states can be explicitly parameterized (Acín *et al.*, 2000).

Again, all these algorithms can be easily implemented and they have properties similar to the one discussed before.

II. PROVING DISTILLABILITY OF QUANTUM STATES

Let us now explain the criteria that were used for proving distillability of the experimentally generated quantum states.

A. Bipartite distillability

For the one qubit vs. three qubits partitions (2×8), it is known that a quantum state in a $2 \times N$ system is distillable, if it has a negative partial transpose (Dür *et al.*, 2000). Therefore, distillability in this system can directly be checked.

For the two qubits vs. two qubits partitions (4×4) we used the mathematical definition of distillability, which states that a state ϱ on $\mathcal{H}_A \otimes \mathcal{H}_B$ is distillable, iff for some k we can find four states

$$\begin{aligned} |e_i\rangle &\in \underbrace{\mathcal{H}_A \otimes \dots \otimes \mathcal{H}_A}_{k \text{ times}} \text{ for } i \in \{1, 2\} \\ |f_i\rangle &\in \underbrace{\mathcal{H}_B \otimes \dots \otimes \mathcal{H}_B}_{k \text{ times}} \text{ for } i \in \{1, 2\} \end{aligned} \quad (8)$$

such that for $|\psi\rangle = \alpha|e_1\rangle|f_1\rangle + \beta|e_2\rangle|f_2\rangle$ the estimate

$$\langle\psi|(\varrho^{T_B})^{\otimes k}|\psi\rangle < 0. \quad (9)$$

holds (Horodecki *et al.*, 1998). For $k = 1$ we searched numerically for the desired $|\psi\rangle$, and if this can be found, the state must be distillable.

B. Entanglement superactivation

Entanglement superactivation is a quantum information processing task, which can work also for the Smolin state as a bound entangled state. Consider two copies of a four-qubit state ϱ which is distributed among five parties as

$$\varrho_{\text{total}} = \varrho^{ABCD} \otimes \varrho^{ABCE}, \quad (10)$$

that is, the parties A, B , and C hold two qubits each, while the parties D and E have only one. In this situation, it was shown that if ϱ is a Smolin state, then the five parties can create a Bell state between D and E by local operations and classical communication only (Shor *et al.*, 2003). The protocol uses a sequence of teleportations.

For the experimental data, we have first applied appropriate local unitary rotations, then this protocol and finally checked with the PPT criterion whether the resulting state between D and E is entangled. We also tested this for arbitrary permutations of the four qubits, since the experimental data are, in contrast to the ideal Smolin state, not permutationally invariant.

III. CHSH-TYPE BELL INEQUALITY

We consider the scenario where each of the 4 parties, labeled j ($j = 1, 2, 3, 4$), can choose between two observables ($O_j^{k_j}$), $k_j = 1, 2$. The CHSH-type Bell inequalities considered here have the form (Augusiak and Horodecki,

2006; Werner and Wolf, 2001; Zukowski and Brukner, 2002):

$$|E(1, 1, 1, 1) + E(1, 1, 1, 2) + E(2, 2, 2, 1) - E(2, 2, 2, 2)| \leq 2, \quad (11)$$

where the correlation function E for the measured quantum state ρ is an average calculated as follows:

$$E(k_1, k_2, k_3, k_N)(\varrho) = \text{Tr} \left[\rho O_{k_1}^{(1)} \otimes O_{k_1}^{(2)} \otimes O_{k_1}^{(3)} \otimes O_{k_N}^{(4)} \right]. \quad (12)$$

For the measured states we maximize the left-hand side of the inequality in Eq. 11, also known as Bell parameter, by varying the observable directions. For the state with $\gamma = 0$, this Bell parameter is 2.21(2), while for the state with $\gamma = 0.06$, the parameter is already 1.47(3).

IV. BISEPARABILITY OF THE STATES WITH $\gamma = 0, 0.06, 0.12$, OR 0.18 .

Applying the separability algorithm to the measured states for these values of γ does not lead to a proof that these states are biseparable. This is due to the fact that the experimental states have some eigenvalues which are practically zero, making the third step of the separability algorithm (Eq. 5) difficult. However, if one takes the state with $\gamma = 0$ and adds 2% of white noise

$$\varrho_{\text{noise}} = 0.98\varrho(\gamma = 0) + 0.02\frac{\mathbb{1}}{16} \quad (13)$$

the algorithm proves that this state ϱ_{noise} is biseparable. It should be noted that the statistical fluctuations of the diagonal elements of $\varrho(\gamma = 0)$ are larger than the amount of noise added. Moreover, if one considers the state consisting of the mixture of all Monte Carlo sample states, the algorithm proves that this state is biseparable. This gives strong evidence for the biseparability of the experimentally generated states.

V. MODEL OF IMPERFECTIONS REVEALS THE OBSERVED DYNAMICS

Several imperfections affect the experimental setup, but to briefly demonstrate that the experimentally observed entanglement dynamics agrees with straightforward calculations, here we choose to only assume imperfect Mølmer-Sørensen operation times (angle θ in $MS(\theta, \phi)$, see report). We consider longer operation times by a small fraction, ε_1 for the 3-out-of-4-entangling operation, $MS((1 + \varepsilon_1)\pi/4, 0)$, and ε_2 for the GHZ-entangling operation, $MS((1 + \varepsilon_2)\pi/2, 0)$. Using the preparation sequence shown in Figure 1 of our report and assuming other operations are perfectly realized, we calculate an expected initial state. Upon decohering this imperfect initial state in two steps, as described in the report, we observe the dynamics of entanglement resembling our measurements, as illustrated here in Figure 1.

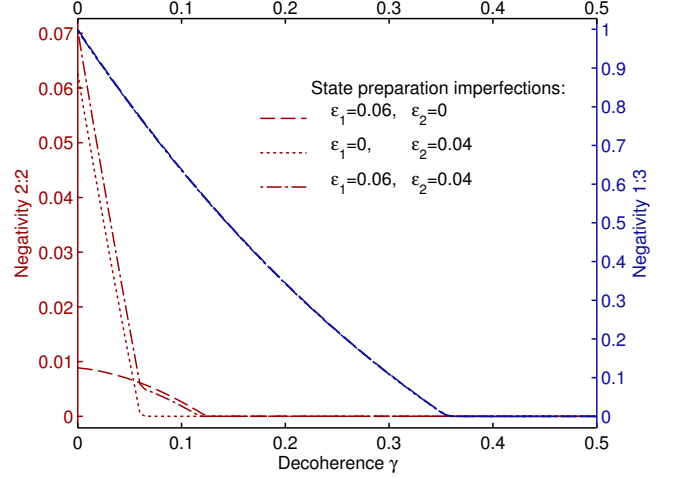


FIG. S1 Negativity for the 2:2 bipartition (left axis) and 1:3 bipartition (right axis) as a function of partial decoherence for the shown imperfections (see text). The imperfections have no effect on the dynamics of $N_{1:3}$. The negativity is the same for all permutations of each bipartition due to the symmetry of the initial state.

VI. QUANTUM STATE RECONSTRUCTION AND STATISTICS

Physical states were tomographically reconstructed via maximum likelihood estimation (MLE) (Jezek *et al.*, 2003). On the four qubits, we performed $3 \times 3 \times 3 \times 3 = 81$ measurements by iterating the measurement of the expectation values of σ_x , σ_y , and σ_z on each qubit. For each state, the number of copies used per state are shown in Table I. Tomographic data were acquired in less than 5.5 hours for each state. Full tomographic sets of 200-250 copies per measurement were acquired iteratively to keep track of potential drifts in the experimental setup.

Error analysis was calculated via Monte Carlo simulations over the multinomially distributed measurement outcomes of the state tomography. For each state, 200 Monte Carlo samples were generated and reconstructed via MLE.

References

- Acín, A., *et al.*, 2000, Phys. Rev. Lett. **85**(7), 1560.
- Acín, A., *et al.*, 2001, Phys. Rev. Lett. **87**(4), 040401.
- Augusiak, R., and P. Horodecki, 2006, Phys. Rev. A **74**, 010305.
- Blume-Kohout, R., 2006, arXiv:quant-ph/0611080.
- Braunstein, S., *et al.*, 1999, Phys. Rev. Lett. **83**(5), 1054.
- Dür, W., J. I. Cirac, M. Lewenstein, and D. Bruß, 2000, Phys. Rev. A **61**, 062313.
- Dür, W., G. Vidal, and J. Cirac, 2000, Phys. Rev. A **62**(6), 062314.
- Gurvits, L., and H. Barnum, 2002, Phys. Rev. A **66**(6), 062311.
- Gurvits, L., and H. Barnum, 2005, Phys. Rev. A **72**(3), 032322.

- Hildebrand, R., 2006, arXiv:quant-ph/0601201 .
- Horodecki, M., P. Horodecki, and R. Horodecki, 1998, Phys. Rev. Lett. **80**, 5239.
- Hulpke, F., and D. Bruß, 2005, J. Phys. A **38**, 5573.
- Jezek, M., J. Fiurasek, and Z. Hradil, 2003, Phys. Rev. A **68**(1), 012305.
- Kendon, V., K. Życzkowski, and W. Munro, 2002, Phys. Rev. A **66**(6), 062310.
- Navascués, M., M. Owari, and M. B. Plenio, 2009, Phys. Rev. Lett. **103**(16), 160404.
- Shor, P. W., J. A. Smolin, and A. V. Thapliyal, 2003, Phys. Rev. Lett. **90**(10), 107901.
- Spedalieri, F., 2007, Phys. Rev. A **76**(3), 032318.
- de Vicente, J. I., 2007, Quantum Inf. Comput. **7**(7), 624.
- Werner, R. F., and M. M. Wolf, 2001, Phys. Rev. A **64**, 032112.
- Zukowski, M., and C. Brukner, 2002, Phys. Rev. Lett. **88**, 210401.
- Zyczkowski, K., *et al.*, 1998, Phys. Rev. A **58**, 883.

TABLE I Negativity and smallest eigenvalue of the partial transpose of measured states for every bipartition.

$\gamma =$		2:2 & 1:3 entangled				Bound Entangled			Fully Separable		single ^a
		0.00	0.06	0.12	0.18	0.24	0.32	0.35	0.47	0.60	0.43
$N_{2:2}$	AB:CD	0.033(5)	0.046(6)	0.017(5)	0.009(5)	0.000(3)	0	0	0	0	0
	AC:BD	0.041(5)	0.043(6)	0.012(5)	0.007(5)	0.000(3)	0	0	0	0	0
	AD:BC	0.044(5)	0.047(7)	0.013(5)	0.006(5)	0.000(3)	0	0	0	0	0
$\min(\text{eig}(\rho^{\text{T}_{2:2}}))$	AB:CD	-0.011(2)	-0.016(2)	-0.008(2)	-0.005(2)	0.005(2)	0.020(2)	0.018(3)	0.028(3)	0.043(2)	0.013(2)
	AC:BD	-0.012(2)	-0.016(2)	-0.006(2)	-0.004(2)	0.004(3)	0.019(2)	0.021(2)	0.029(3)	0.045(2)	0.011(2)
	AD:BC	-0.013(1)	-0.015(2)	-0.007(2)	-0.003(2)	0.005(3)	0.022(2)	0.016(3)	0.031(2)	0.043(2)	0.013(2)
$N_{1:3}$	A:BCD	0.715(8)	0.507(14)	0.438(14)	0.335(13)	0.199(11)	0.035(7)	0.021(10)	0	0	0.038(7)
	B:ACD	0.715(8)	0.509(14)	0.440(14)	0.337(12)	0.195(11)	0.032(8)	0.022(10)	0	0	0.039(7)
	C:ABD	0.715(8)	0.510(14)	0.439(14)	0.337(12)	0.197(11)	0.038(8)	0.015(9)	0	0	0.042(7)
	D:ABC	0.716(8)	0.509(14)	0.438(14)	0.337(12)	0.208(11)	0.045(7)	0.028(10)	0	0	0.045(7)
$\min(\text{eig}(\rho^{\text{T}_{2:2}}))$	A:BCD	-0.102(2)	-0.088(2)	-0.077(3)	-0.064(3)	-0.045(3)	-0.015(2)	-0.008(3)	0.019(3)	0.042(2)	-0.011(2)
	B:ACD	-0.104(2)	-0.088(3)	-0.079(3)	-0.063(3)	-0.040(3)	-0.014(2)	-0.008(3)	0.020(3)	0.042(2)	-0.015(2)
	C:ABD	-0.104(1)	-0.087(3)	-0.075(3)	-0.062(3)	-0.042(3)	-0.012(2)	-0.007(3)	0.019(3)	0.042(2)	-0.014(2)
	D:ABC	-0.105(2)	-0.089(2)	-0.079(3)	-0.064(3)	-0.045(3)	-0.016(2)	-0.009(3)	0.018(3)	0.043(2)	-0.014(2)
(state copies)/(81 meas.)		5000	3000	3000	3250	3750	6000	3100	3000	4000	6000

^aBound-entangled state decohered in a single step, see report.

TABLE II Summary of Monte Carlo samples satisfying the tested properties.

Decoherence $\gamma =$	0	0.06	0.12	0.18	0.24	0.32	0.35	0.47	0.60	single
2:2 entangled	200	200	200	200	41 ^a	0	0	0	0	1
2:2 distillable	200	200	194	172	2 ^b	0	0	0	0	0
1:3 entangled	200	200	200	200	200	200	200	0	0	200
1:3 distillable	200	200	200	200	200	200	200	0	0	200
superactivatable	200	200	200	0	0	0	0	0	0	0
biseparable	200 ^c	200 ^c	200 ^c	200 ^c	200	200	200	200	200	200
fully separable	0	0	0	0	0	0	0	0	200	0

^aThese 41 states had a non-positive partial transpose for all permutations of the 2:2 bipartition.^b44 states had a positive partial transpose on every permutation of the 2:2 bipartition (undistillable) and were also 2:2 separable.^cStrong evidence, discussed in text.

TABLE III Absolute value of measured density matrices.

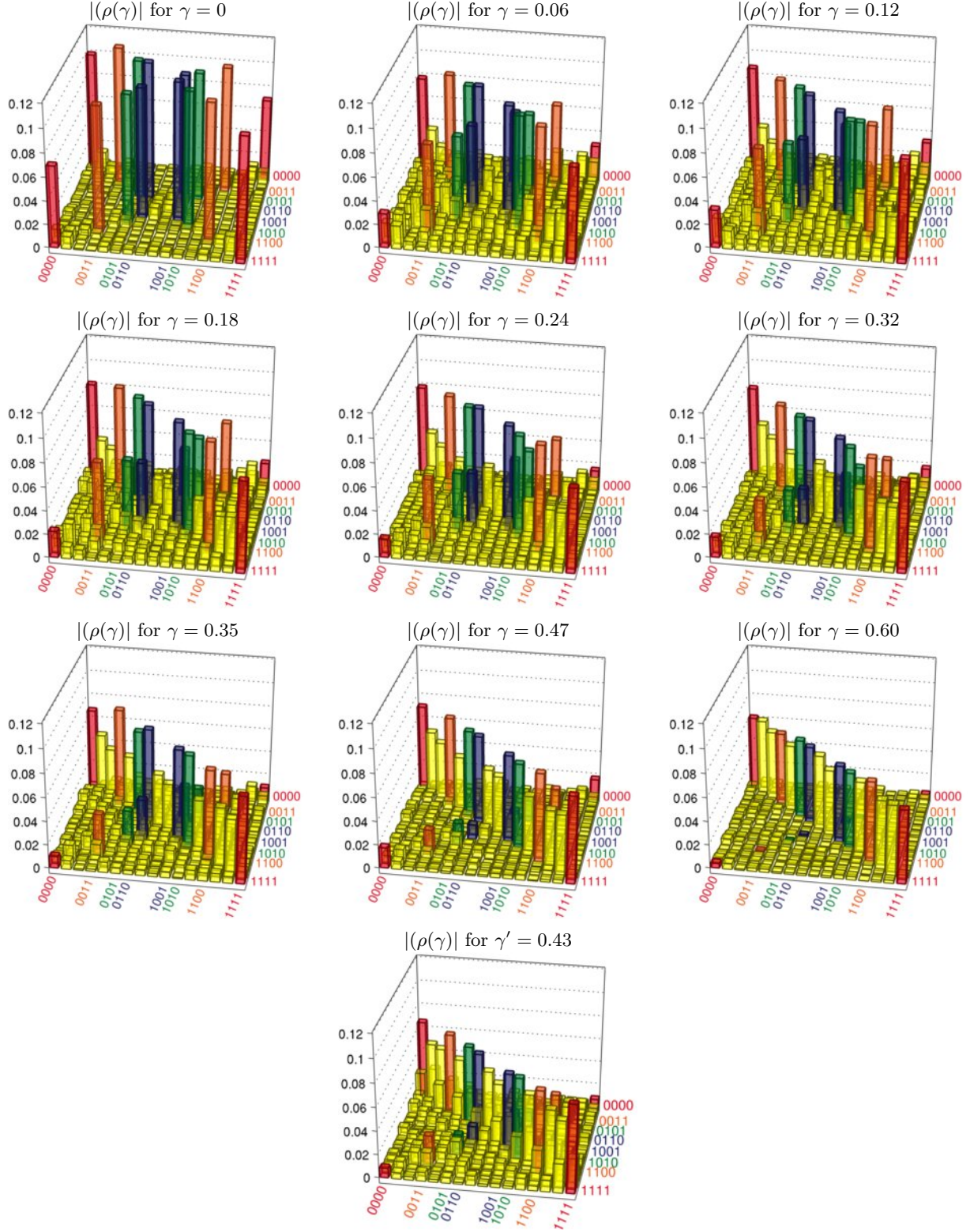


TABLE IV Absolute value of density matrices $\varrho(\gamma)$ calculated by applying local unitaries to the measured states $\rho(\gamma)$ which maximize the amplitudes of their real part. This transformation facilitates visualizing the Smolin components of the states.

